J5.11 **A STUDY OF STABILITY CONDITIONS IN AN URBAN AREA**

Stevens T. Chan* and Julie K. Lundquist
Lawrence Livermore National Laboratory
Livermore, California 94551, USA

1. INTRODUCTION

Accurate numerical prediction of airflow and tracer dispersion in urban areas depends, to a great extent, on the use of appropriate stability conditions. Due to the lack of relevant field measurements or sufficiently sophisticated turbulence models, modelers often assume that nearly neutral conditions are appropriate to use for the entire urban area being simulated. The main argument for such an assumption is that atmospheric stability (as defined by the Richardson number) is determined by both mechanical stresses and buoyant forcing but, for a typical urban setting with a given thermal stability or sensible heat flux, building-induced mechanical stresses can become so dominant to drive the resulting stability toward nearly neutral conditions.

Results from our recent simulations of two Joint URBAN 2003 releases, using a computational fluid dynamics (CFD) model - FEM3MP, appear to support partially the assumption that urban areas tend toward neutral stability. More specifically, based on a model-data comparison for winds and concentration in the near field and velocity and turbulence profiles in the urban wake region, Chan and Lundquist (2005) and Lundquist and Chan (2005) observed that neutral stability assumption appears to be valid for intensive operation period (IOP) 9 (a nighttime release with moderate winds) and also appears to be valid for IOP 3 (a daytime release with strong buoyant forcing) in the urban core area but is less valid in the urban wake region.

Our model, developed under the sponsorship of the U.S. Department of Energy (DOE) and Department of Homeland Security (DHS), is based on solving the three-dimensional, time-dependent, incompressible Navier-Stokes equations on massively parallel computer platforms. The numerical algorithm is based on finite-element discretization for effective treatment of complex building geometries and variable terrain, together with a semi-implicit projection scheme and modern iterative solvers developed by Gresho and Chan (1998) for efficient time integration. Physical processes treated in our code include turbulence modeling via Reynolds Averaged Navier-Stokes (RANS) and Large Eddy Simulation (LES) approaches described in Chan and Stevens (2000), atmospheric stability, aerosols, UV radiation decay, surface energy budgets, and vegetative canopies, etc. Predictions from our model are continuously being verified against measured data from wind tunnel and field experiments. Examples of such studies are discussed in Chan et al. (2001, 2004), Chan and Leach (2004), Calhoun et al. (2004, 2005), and Humphreys et al. (2004).

In this study, the stability conditions associated with two more of the Joint URBAN 2003 releases are investigated. Through a model-data comparison of the wind and concentration fields, observed buoyancy production in the urban wake region, together with predicted values of turbulence kinetic energy (TKE) in various regions of the computational domain, a more definitive characterization of stability conditions associated with the simulated releases is presented.

In the following, we first discuss briefly the field experiments being simulated, then present sample results from a model-data comparison for both the wind and concentration fields, examine the predicted TKE field and the observed buoyant forcing relative to the total TKE in the urban wake, and finally offer a few concluding remarks including the resulting stability conditions of the simulated releases**.**

2. THE JOINT URBAN 2003 FIELD STUDY

In order to provide quality-assured, high-resolution meteorological and tracer data sets for evaluation and validation of indoor and outdoor urban dispersion models, the U.S. DHS and DoD – Defense Threat Reduction Agency co-sponsored a series of dispersion experiments, named Joint URBAN 2003 (Allwine et al., 2004), in Oklahoma City (OKC), Oklahoma, during July 2003. These experiments are complementary to the URBAN 2000 experiments (Allwine et al., 2002) conducted in Salt Lake City in that they provide another comprehensive field data set for the evaluation of CFD and other dispersion models. In contrast to the URBAN 2000 experiments, which were conducted entirely at night, these experiments took place during daytime and nighttime to include both convective and stable atmospheric conditions. A total of ten IOPs were conducted and SF_6 in the form of puffs or continuous sources were released over 6 daytime and 4 nighttime episodes.

Many wind and concentration sensors were used to collect wind and SF_6 data over both long and short time-averaging periods. In addition to measurements

*Corresponding author address: S. T. Chan, Lawrence Livermore National Laboratory, P.O. Box 808, L-103, Livermore, CA 94551, e-mail: **schan@llnl.gov.**

near the surface, wind and concentration profiles adjacent to the outside walls of several buildings were also taken. Furthermore, a pseudo-tower, supported by a 90-m crane and fitted with sonic anemometers at eight levels, was deployed downwind at about 750 m from downtown OKC for turbulence observations. In one nocturnal case, balloons were deployed close to the tracer release area. Many of the released balloons exhibited quick ascents from ground level to the top of buildings, implying highly convective conditions.

3. MODAL-DATA COMPARISON

In this study, airflow and dispersion simulations for the first continuous release of IOPs 2 and 8, a daytime and a nighttime release respectively, were performed. In each case, SF_6 was released near the ground as a point source for 30-min, with a release rate of 5.0 g/s for IOP 2 and 3.1 g/s for IOP 8. Shown in Fig. 1 are the footprints of buildings in the central business district of OKC, with the Westin release location indicated by the red dot. The tallest building in the area is approximately 120-m high and the average building height of the area is ~30 m.

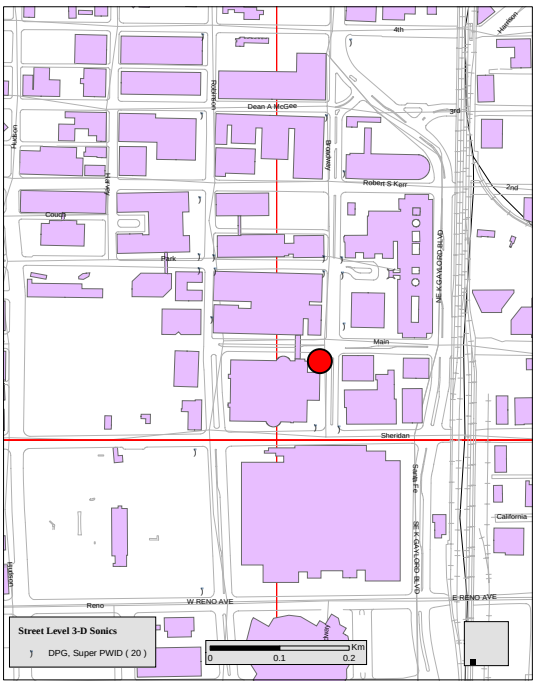

Fig. 1. Footprints of buildings in the central business district of Oklahoma City and the Westin release location (red dot) for IOP 2 and IOP 8.

In the numerical simulations, a domain size of 1,030 m x 3,010 m x 425 m (in lateral, longitudinal, and vertical directions) was employed. A graded mesh consisting of 201 x 303 x 45 grid points, with a minimal grid spacing of ~1 m near the ground surface, was used. Most of the buildings within 500 m of the release point were explicitly resolved and the remaining buildings were treated as virtual buildings.

Steady logarithmic velocity profiles were used as inflow boundary conditions. These profiles were created, based on the 15-minute averaged wind speeds and directions from the PNNL sodar located approximately 2 km SSW of downtown OKC and the hourly averaged data from the weather station on the rooftop of St. Anthony's hospital at ~1.5 km NW of downtown OKC. The estimated wind speed is 5 m/s at z=50 m for both IOPs and the estimated wind direction is 215^o for IOP 2 and 155^o for IOP 8, respectively.

For each simulated release, a quasi-steady state flow field was established after ~15 minutes of simulated time prior to the start of the dispersion simulation. The release of SF_6 was modeled as a continuous source over a small area (covered by 2 x 2 cells on the ground surface) at a constant release rate and dispersion results indicate steady state was reached in about 20 minutes of simulated time. For both cases, the RANS approach with a non-linear eddy viscosity (NEV) turbulence model (Gresho and Chan, 1998) was used and neutral atmospheric stability was assumed.

In the following, model predictions of flow and concentration in the near and intermediate regions of the release point are presented and compared with observed data. For brevity, only major results are presented and compared herein. Several of the statistical performance measures recommended by Hanna, et al. (2005) are used to indicate the performance of our model. They are: the factor of two or five (FAC2 or FAC5), fractional bias (FB), the geometric mean bias (MG), and the normalized mean square error (NMSE). For differences in angles between predicted and measured wind vectors, the formula of scaled angle differences (SAA) with larger vectors carrying more weights, devised by Calhoun, et al. (2004), is used.

3.1 IOP 2

Airflow in urban areas is extremely complex, with features such as flow separations, local stagnation regions, eddies of various size, and high velocity jets in street canyons. These features were all observed in our model simulations. Due to space limitations, the simulated flow field is not presented here, however, a quantitative model-data comparison of wind vectors at a number of locations is presented. In Fig. 2, the predicted wind vectors in the downtown area are compared with the 30-min averaged data measured by Dugway Proving Ground (DPG) PWIDS. In general, the agreement between model predictions and field observations is very good. The statistical performance measures are: SAA=15, FAC2=0.6, FB=-0.04, MG=0.71, and NMSE=0.41, respectively.

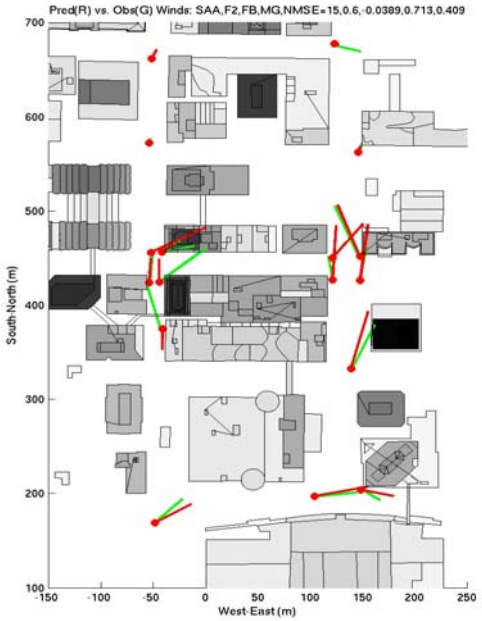

Fig. 2. Comparison of predicted wind vectors (red arrows) against 30-min averaged data (green arrows) measured by DPG PWIDS on z=8 m plane for IOP 2.

In Fig. 3, predicted concentration patterns are shown and compared against the observed 15-minute averages obtained from Blue Box data, which are the small squares with the same color scheme. In addition to being dispersed downwind and slightly upwind, the plume is seen to spread more to the east and veers to NNE beyond the downtown area. Except for missing narrowly two sensors with lower concentrations upwind of the source, the predicted concentrations generally agree well with the measured data. The statistical performance measures are: FAC5=0.63, FB=-0.56, MG=0.79, and NMSE=1.14, respectively.

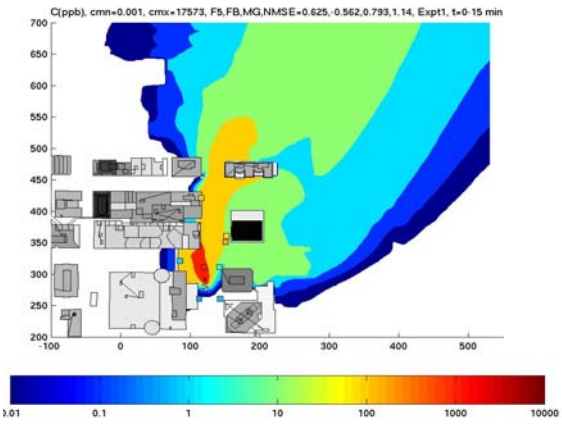

Fig. 3. Predicted concentration patterns and comparison with Blue Box data measured in the source area for IOP 2.

The predicted concentrations (blue line) along Broadway Avenue (at x=122 m in Fig. 3) are compared against the time-averaged data in Fig.4, with red circles for data averaged over t=0-15 minutes and green circles for data averaged over t=15-30 minutes. Because of the relatively short duration of the release and sparseness of measured data, it is considered more appropriate to compare model predictions against data obtained for both averaging times. The agreement is generally very good except that the predicted concentrations are much lower than observed for downwind distance > 1,000 m. These results suggest the predicted plume has veered more to the east than observed in the urban wake region and beyond. The unsteady nature of the actual incoming flow could have caused the plume to meander, thus resulting in a wider plume. In addition, the crane data (in the upper right panel of Fig. 11) implies that the incoming mean wind direction assumed in the numerical simulation was probably 10 to 15 degrees greater than the actual mean wind direction, which could also make the predicted plume veer too much to the east in the urban wake region and beyond.

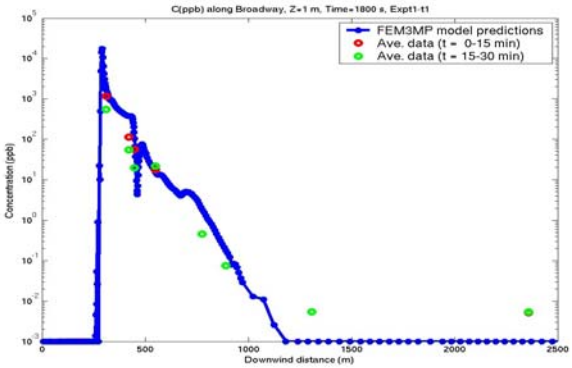

Fig. 4. Comparison of predicted versus observed concentrations along Broadway Avenue for IOP 2. Blue line – model predictions with NEV and neutral stability; red and green circles - observed data.

3.2 IOP 8

In this subsection, sample flow and dispersion results from simulations of the IOP 8 release are presented and compared with available data in the next four figures. In Fig. 5, the predicted wind vectors and speeds (color contours) in the OKC downtown area are depicted to illustrate the complex features of airflow in the area. Such features include stagnations in front of buildings, flow separations on the sides, jetting in street canyons, and various building wakes. In addition, there are obvious converging and diverging flows in the source area (the southeast quadrant of the figure). As a result, the plume spreads considerably in the upwind and lateral directions as will be shown in Fig. 7.

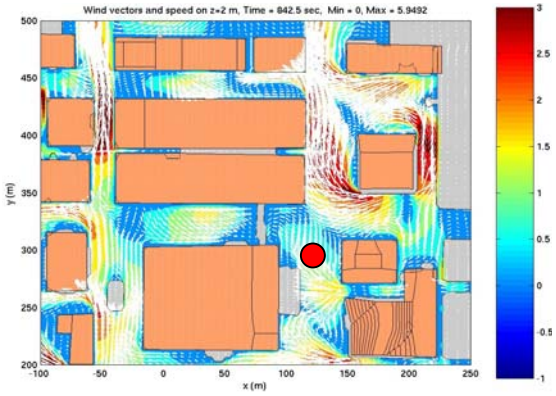

Fig. 5. Predicted wind vectors and wind speeds (color contours) on z=2 m plane for IOP 8, illustrating the complexity of airflow in the OKC downtown area. Red dot is the source location.

In Fig. 6, predicted wind vectors in the downtown area are compared with the 30-min averaged data measured by DPG PWIDS. Again, the overall agreement between model predictions and field measurements is very good. The statistical performance measures are similar to those in the previous case: SAA=34, FAC2=0.84, FB=0.11, MG=1.21, and NMSE=0.13. A close examination of Figs. 2 and 6 reveals the significant differences in both wind speeds and directions, which are solely due to the difference in the incoming wind direction from 215^{o} to 155^{o}.

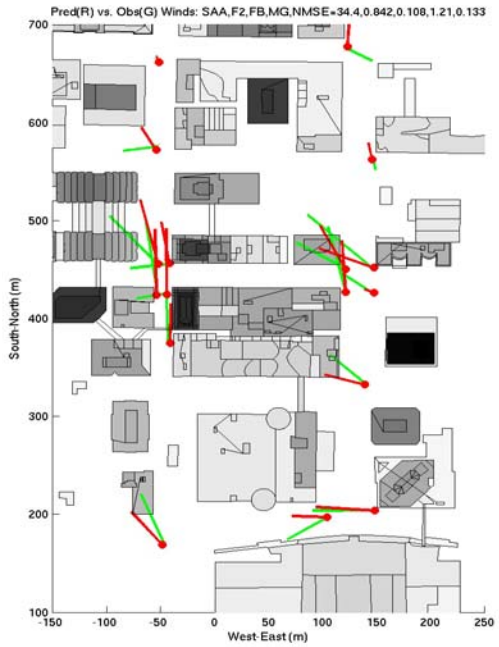

Fig. 6. Comparison of predicted wind vectors (red arrows) against 30-min average data (green arrows) measured by DPG PWIDS on z=8 m plane for IOP 8.

In Fig. 7, predicted concentration patterns in the downtown area are shown and compared against 15-minute averaged Blue Box data. Again, the predicted results generally agree very well with the observed data. In particular, the model was able to predict the significant upwind and lateral spread indicated by the measured data. The statistical performance measures are: FAC5=0.54, FB=-0.76, MG=1.3, and NMSE=3.56, respectively.

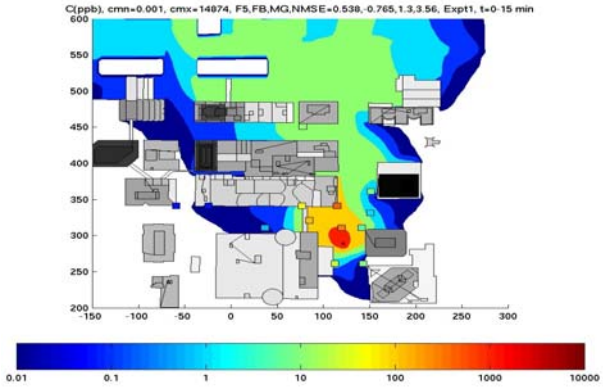

Fig. 7. Predicted concentration patterns and comparison with Blue Box data measured in the source area for IOP 8.

In Fig. 8, the predicted concentrations (blue line) along Broadway Avenue at x=122 m in Fig. 7) are compared against the time-averaged data. Again, because of the relatively short duration of the release and sparseness of measured data, model predictions are compared against data obtained for both averaging times. The agreement is mostly within a factor of 3 except for downwind distance >1,000 m, wherein the predicted values are much too low. The discrepancies could probably be explained by the omission of the time variations in the incoming flow (thus no plume meandering) and the incoming mean wind direction assumed in the numerical simulation was probably 10^{o} too small as suggested by the crane data in the upper right panel of Fig. 12.

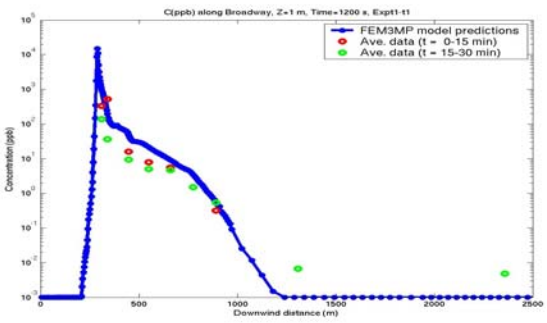

Fig. 8. Comparison of predicted versus observed concentrations along Broadway Avenue for IOP 8. Blue line – model predictions with NEV and neutral stability; red and green circles - observed data.

4. ANALYSIS OF TKE AND CRANE DATA

In this section, the average values of predicted TKE at various locations within the computational domain are examined. Turbulence data collected on the crane (in the urban wake region) were also analyzed to construct winds and TKE profiles in the area. These results are considered together to assess the stability conditions associated with the releases simulated in this study.

In Figs. 9 and 10, predicted TKE contours in downtown OKC and the urban wake region on the z=32 m plane (~average building height of OKC downtown area) are displayed. These pictures indicate, in both cases, significant TKE due to building-induced turbulence was generated. It is interesting to note, at this height, regions with the highest turbulence intensity are on the edges of the central business area, because these locations are close to clusters of many taller buildings in the area. Within the central business area, TKE levels are considerably lower in the relatively quiescent region occupied by the weaker building wakes.

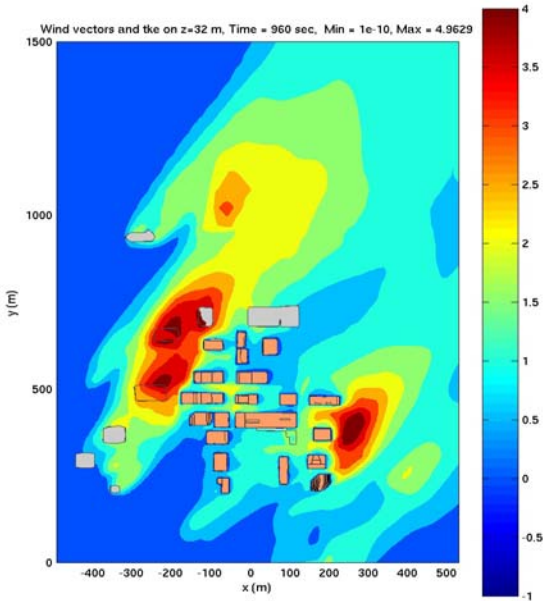

Fig. 9. Predicted contours of turbulence kinetic energy on z=32 m plane for IOP 2.

As a rough estimate of TKE intensity in various zones of the computational domain, averaged TKE values are computed for three somewhat arbitrarily defined zones. The zones are defined as: upwind (y=-400 m to 0), urban (y=200 m to 1000 m), and downwind (y=2000 m to 2600 m). The same crosswind extent from x=-450 m to 450 m and the same height of 200 m are used in all three zones. The averaged TKE values are tabulated below:

IOP	Upwind TKE	Urban TKE	Downwind TKE
2	0.20	1.09	0.32
8	0.22	1.07	0.27

The above values indicate turbulence intensity in the urban area is about 5 times that at upwind and about 4 times that at downwind locations. Due to turbulence transport from the urban area, turbulence intensity in the downwind area is, as expected, somewhat higher than that in the upwind region. Assuming the averaged TKE value upwind is representative of the turbulence level in the rural area, the above estimates suggest that building-induced mechanical stresses have caused the turbulence intensity to increase by as much as four times in the urban area. The two sets of values also indicate the incoming wind flow direction is not a strong factor in determining the averaged TKE values in different zones, at least for the two wind directions considered herein.

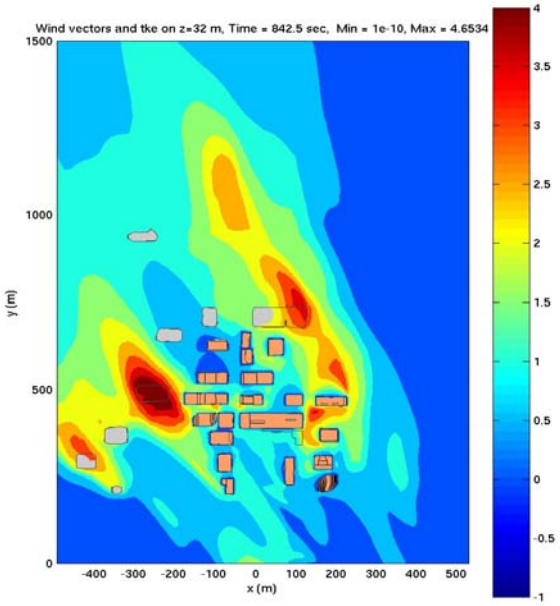

Fig. 10. Predicted contours of turbulence kinetic energy on z=32 m plane for IOP 8.

During the JU2003 experiment, a pseudo-tower at about 750 m from downtown OKC (at x = -200 m and y=1,200 m in Fig. 10) was deployed for turbulence observations. The observed data was analyzed for model-data comparison and also used for assessing the neutral stability conditions assumed in the present simulations.

In Fig. 11, a comparison of predicted versus observed profiles of four variables at the crane station

for IOP 2 is presented. Included in the comparison are profiles of wind speed, wind direction, friction velocity, and TKE. The observed profiles have been obtained by various averaging-time intervals, ranging from 300 to 1,800 sec. Among all the averaging times, results from the 1,800 sec interval (red lines) are considered the most appropriate and will be used in all subsequent comparison.

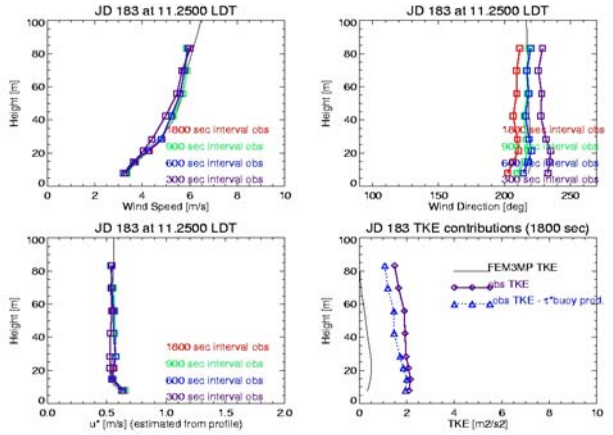

Fig. 11. Comparison of predicted versus observed profiles at crane station for IOP 2: wind speed (UL), wind direction (UR), friction velocity (LL), and TKE (LR). Black lines – predicted profiles; color lines – time-averaged profiles using various time intervals.

As is seen in the figure, there is an excellent agreement between the predicted and observed profiles for both the wind speed (upper left panel) and friction velocity (lower left panel). The agreement between predicted and observed wind direction profile is fairly good, with the predicted wind direction being greater than the observed values (red line) by about 10 to 15 degrees (more westerly than observed).

In the lower right panel, the purple line is the (total) observed TKE profile obtained from using a 1,800 sec averaging time. The blue line is the TKE profile with the buoyant production contribution removed, against which the predicted profile should be compared. The buoyant contribution is calculated from the buoyant production of TKE multiplied by a turbulent time scale τ determined from the quotient of TKE over dissipation rate, following the model of Zeierman and Wolfshtein (1986). Dissipation rate was calculated using the inertial dissipation method (Piper and Lundquist, 2004), assuming isotropy and using a 30-minute time series at each level of the crane. The two observed TKE profiles suggest that buoyant production contributes only between 5% and 25% of the total TKE budget.

The predicted and observed TKE profiles have very similar shapes, however, the predicted TKE values are at most only 25% of the observed values. Such large discrepancies are probably due to the fact that a greater incoming wind direction, by 10-15^{o} as suggested by the crane data in the upper right panel, was used in the numerical simulation. As a result, the predicted urban wake has veered too much to the east and only the edge of the urban wake was near the crane, as can be seen in Fig. 9.

In Fig. 12, a comparison of predicted versus observed profiles of four variables, including wind speed, wind direction, friction velocity, and TKE, at the crane station for IOP 8 is presented. There is a good agreement between the predicted and observed profiles for both the wind speed (upper left panel) and friction velocity (lower left panel) in the first 25 m above ground level (AGL), above which the agreement is only fair. Model predictions for both wind speed and friction velocity at the crane top is only approximately 65% of the observed values. In addition to possible errors in estimated inflow wind direction, as in IOP 2 above, the discrepancies between observations and simulations for IOP 8 could be due to larger scale flow processes not currently accounted for in our simulation. A companion paper, Lundquist (2005), discusses the occurrence of a nocturnal low-level jet on the night of IOP 8 based on data from the pseudo-tower and the PNNL boundary-layer wind profiler 2 km SSW of the OKC urban core. Shear generated by the low-level jet could be responsible for the vertical transport of momentum from upper levels into the lower levels simulated here, thereby increasing wind speed, friction velocity, and TKE. Because our simulations exclude the possibility of vertical transport of momentum from outside the simulation domain, such processes are not included in the simulations and could therefore explain some of the discrepancies between observations and simulations.

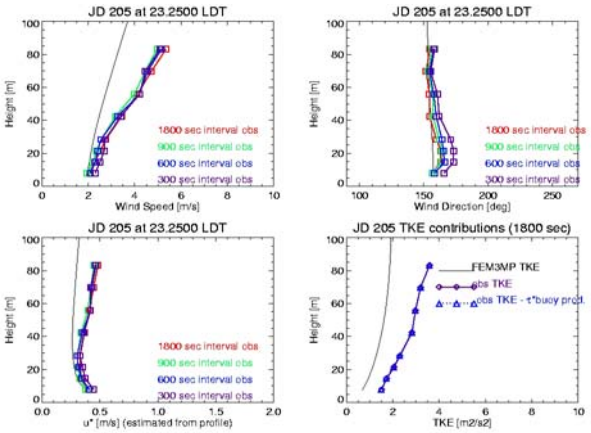

Fig. 12. Comparison of predicted versus observed profiles at crane station for IOP 8: wind speed (UL), wind direction (UR), friction velocity (LL), and TKE (LR). Black lines – predicted profiles; color lines – time-averaged profiles using various time intervals.

In the upper right panel, the predicted and observed profiles for the wind direction are compared. The agreement between predicted and observed profiles is

generally good except for z=15 to 30 m, with the largest under-prediction of the angle by ~10^{o} near z=15 m AGL.

In the lower right panel, profiles of observed TKE (purple line), observed TKE without buoyant production (blue line), and predicted TKE (black line) are displayed. The two observed TKE profiles suggest that buoyant production, in this case, is negligible. The predicted and observed profiles have similar shapes, however, the predicted values are only about 55% of those observed. Again, the possibility of a nocturnal jet present during the release is a plausible explanation for the higher TKE being observed. The slightly inaccurate incoming flow direction used in the numerical simulation could also contribute to some of the discrepancies.

5. CONCLUSIONS

In this paper, the FEM3MP model has been further evaluated using observed winds in downtown OKC, observed wind and TKE profiles at the crane station in the urban wake region, and concentration data from IOPs 2 and 8 of the Joint URBAN 2003 experiment. Our model predictions for both IOPs, regarding winds, concentrations, profiles of wind speed, wind direction, and friction velocity, are generally very consistent and compare reasonably well with the field observations.

At the crane station, although the shapes of the predicted TKE profiles are similar to those observed in both cases, the predicted turbulence intensities are too low. For IOP 2, the predicted turbulence levels are at most only 25% of the observed values, which could be due to inadequate specification of the incoming flow direction (by 10 to 15 degrees). For IOP 8, the predicted TKE values are only about 55% of the observed values. The possible presence of a nocturnal low-level jet during this nighttime release is a plausible explanation for the higher TKE values observed.

Our rough estimates of the average TKE values in various zones of the computational domain suggest that building-induced turbulence can cause the average turbulence intensity in the urban area to increase by as much as four times but only cause a slight increase in TKE levels in the urban wake region. The average TKE values are almost independent of the two wind directions considered in this study.

The TKE budget at the crane station (in the urban wake region) has been analyzed to determine the importance of buoyant forcing relative to the total TKE. For IOP 2 (a daytime release), the buoyancy production contributes about 25% to the total TKE budget in the region. For IOP 8 (a nighttime release), the contribution of buoyancy production/ destruction to the total TKE budget in the same region is negligible.

Considering the fact that buoyancy effects are negligible during the nighttime release (IOP 8), the assumption of neutral stability is vindicated. For the daytime release (IOP 2), although the buoyancy production could contribute up to 25% of the TKE budget, the assumption of neutral stability in the urban area is still valid because building-induced turbulence is dominant (~4 time increase in TKE) in the area. However, in the urban wake region and further downwind, the levels of building-induced turbulence have greatly subsided, hence the assumption of neutral stability is less valid and should be considered in the flow and dispersion simulation.

6. REFERENCES

Allwine, K., J. Shinn, G. Streit, K. Clawson, and M. Brown, 2002: Overview of URBAN 2000, Bulletin of the American Meteorological Society 83 (4), 521-536.

Allwine, K., M. Leach, L. Stockham, J. Shinn, R. Hosker, J. Bowers, and J. Pace, 2004: Overview of Joint Urban 2003, AMS Annual Meeting, Seattle, WA, Jan. 11-15, 2004.

Calhoun, R., F. Gouveia, J. Shinn, S. Chan, D. Stevens, R. Lee, and J. Leone, 2005: Flow Around a Complex Building: Comparisons between Experiments and a Reynolds-Averaged Navier-Stokes Approach, Vol. 43, JAM, 696-710.

Calhoun, R., F. Gouveia, J. Shinn, S. Chan, D. Stevens, R. Lee, and J. Leone, 2005: Flow Around a Complex Building: Experimental and Large-eddy Simulation Comparisons, Vol. 44, JAM, 571-590.

Chan, S. and D. Stevens, 2000: An Evaluation of Two Advanced Turbulence Models for Simulating the Flow and Dispersion Around Buildings, The Millennium NATO/CCMS Int. Tech. Meeting on Air Pollution Modeling and its Application, Boulder, CO, May 2000, 355-362.

Chan, S., D. Stevens, and W. Smith, 2001: Validation of Two CFD Urban Dispersion Models Using High Resolution Wind Tunnel Data, 3rd Int. Sym. on Environ, Hydraulics, ASU, Tempe, AZ, Dec. 2001, 107.

Chan, S., T. Humphreys, and R. Lee, 2004: A Simplified CFD Approach for Modeling Urban Dispersion, AMS Annual Meeting, Seattle, WA, Jan. 11-15, 2004.

Chan, S., and M. Leach, 2004: Large Eddy Simulation of an URBAN 2000 Experiment with Various Time-dependent Forcing, 5th Symposium on the Urban Environment, Vancouver, Canada, Aug. 23-27, 2004.

Chan, S. and J. Lundquist, 2005: A Verification of FEM3MP Predictions Against Field Data from Two Releases of the Joint URBAN 2003 Experiment, 9th GMU Conference on Atmospheric Transport and Dispersion Modeling, Fairfax, VA, July 18-20, 2005.

Gresho, P. and S. Chan, 1998: Projection 2 Goes Turbulent – and Fully Implicit, Int. J. of Comp. Fluid Dynamics, 9, 249-272.

Hanna, S., O. Hansen, and S. Dharmavaram, 2005: FLACS CFD Air Quality Model Performance Evaluation with Kit Fox, Prairie Grass, MUST, and EMU Observations, Submitted to Atmospheric Environment, 2005.

Humphreys, T., S. Chan, R. Lee, and Eric Peterson, 2004: A Validation of Simplified CFD Approach for Modeling Urban Dispersion with Joint Urban 2003 Data, AMS 5th Symposium on the Urban Environment, Vancouver, Canada, Aug. 23-27, 2004.

Lundquist, J. K., 2005: Interaction of Nocturnal Low-Level Jets with Urban Geometries as seen in Joint URBAN 2003 Data, AMS 6th Symposium on the Urban Environment, Atlanta, Georgia, Jan 29 – Feb 2, 2006 (this volume).

Lundquist, J. and S. Chan, 2005: Analysis of Joint URBAN 2003 Wind and Turbulence Profiles and Comparison with FEM3MP Simulations, 9th GMU Conference on Atmospheric Transport and Dispersion Modeling, Fairfax, VA, July 18-20, 2005.

Piper, M.D., and J.K. Lundquist, 2004: Surface Layer Turbulence Measurements during a Frontal Passage, J. Atmos. Sci., 61, 1768-1780.

Zeierman, S., and M. Wolfshtein, 1986: Turbulent Time Scale for Turbulent-Flow Calculations, AIAA Journal, 24, 1606-1610.

ACKNOWLEDGEMENTS

This work was performed under the auspices of the U.S. Department of Energy by the University of California, Lawrence Livermore National Laboratory under contract No. W-7405-Eng-48.